Hookworm-derived small molecule extracts suppress pathology in a mouse model of colitis and inhibit secretion of key inflammatory cytokines in primary human leukocytes

Phurpa Wangchuk[a*], Constantin Constantinoiu[b], Konstantinos A. Kouremenos[c], Luke Becker[a], Linda Jones[a], Catherine Shepherd[a], Geraldine Buitrago[a], Paul Giacomin[a], Norelle Daly[a], Malcolm J. McConville[c], Rachael Y. M. Ryan[a], John J. Miles[a], Alex Loukas[a*]

[a]Centre for Biodiscovery and Molecular Development of Therapeutics, Australian Institute of Tropical Health and Medicine, James Cook University, Cairns, QLD 4878, Australia.

[b]College of Public Health, Medical and Veterinary Sciences, Centre for Biosecurity in Tropical Infectious Diseases, James Cook University, Townsville, QLD 4878, Australia.

[c]Metabolomics Australia, Bio21 Molecular Science and Biotechnology Institute, University of Melbourne, 30 Flemington Road, Parkville, VIC 3010, Australia.

Running Head: Anti-inflammatory hookworm small molecules

*Corresponding author: Prof. Alex Loukas (alex.loukas@jcu.edu.au), Australian Institute of Tropical Health and Medicine, Building E4, James Cook University, McGregor Rd., Smithfield, QLD 4878, Australia; Dr Phurpa Wangchuk (phurpa.wangchuk@jcu.edu.au), Australian Institute of Tropical Health and Medicine, Building E4, James Cook University, McGregor Rd., Smithfield, QLD 4878, Australia

ABSTRACT Iatrogenic hookworm therapy shows promise for treating disorders that result from a dysregulated immune system, including inflammatory bowel disease (IBD). Here we use a metabolomics approach to characterize the non-protein small molecule complement of hookworms. Gas chromatography-mass spectrometry and liquid chromatography-mass spectrometry analyses of somatic tissue extracts revealed the presence of 52 polar metabolites and 22 non-polar components including short chain fatty acids (SCFA). Several of these small metabolites, notably the SCFA, have been shown to have anti-inflammatory properties in various diseases, including IBD. Using a murine model of colitis and human peripheral blood mononuclear cells, we demonstrate that somatic tissue extracts of the hookworm *Ancylostoma caninum* contain small molecules with anti-inflammatory activities. Of the five extracts tested, two of them significantly protected mice against T cell-mediated immunopathology and weight loss in a chemically-induced colitis model. Moreover, one of the anti-colitic extracts suppressed *ex vivo* production of inflammatory cytokines from primary human leukocytes. While the origin of the SCFA (parasite or host microbiota-derived) present in the hookworm somatic tissue extracts cannot be ascertained from this study, it is possible that *A. caninum* may be actively promoting an anti-inflammatory host microbiome by facilitating immune crosstalk through SCFA production.

KEYWORDS Hookworm; *Ancylostoma caninum*; Somatic tissue extracts; Ulcerative colitis; Short chain fatty acids; GC-MS; Metabolome

Inflammatory Bowel Disease (IBD) is associated with chronic inflammation of the digestive tract, and primarily includes ulcerative colitis (UC) and Crohn's disease (CD). The etiology of IBD is not well established but it is usually characterized by inflammation, loss of appetite and weight, chronic diarrhea, bloody stools, fever, rectal bleeding, abdominal pain, fatigue, and anemia (1-3). IBD has been linked to many extra-intestinal manifestations (4) and implicated with mental health problems (5). Current treatments for IBD include, 5-aminosalicylates, glucocorticosteroids, immunomodulators and biologics, and proctocolectomy as a last resort when drug treatment fails. Many of these drugs are often associated with side-effects and various postoperative complications (6, 7). Frontline biologics such as treatment with anti-TNF monoclonal antibodies are only efficacious in some patients and treatment does not result in long term cure (8). Failure of these frontline treatments is associated with elevated risk of colon cancer, and can result in the need for surgical removal of the colon (partial or full). There is therefore an urgent need for new and effective anti-inflammatory drugs to treat IBD.

Guided by millennia of host-parasite co-evolution, we (9-13) and others (14-16) have demonstrated the therapeutic properties of experimental hookworm infection to treat gastrointestinal (GI) inflammatory diseases. Hookworms resident in the human GI tract induce tolerogenic dendritic cells and regulatory T cells which produce suppressor cytokines that keep inflammatory T cells and their effector molecules in check (17, 18). While iatrogenic hookworm therapy shows promise for treating numerous inflammatory diseases in humans, it presents many challenges including apprehension by the patient to readily accept such a radical intervention, safety concerns and regulatory hurdles. In order to circumvent these limitations, we have investigated whether the immunomodulatory properties of hookworms are due to specific metabolites in the parasite's somatic tissue or excretory/secretory products (ESP). Administration

of hookworm ESP to mice protected against inflammation and weight loss in two different mouse models of chemically-induced colitis - the T cell-dependent trinitrobenzene sulfonic acid (TNBS) model (19) and the T cell-independent dextran sulfate sodium (DSS) model (20). We previously characterized the protein constituents (>10 kDa) of hookworm ESP (21), and recently identified a single protein, *Ac*-AIP-2, which in recombinant form displays immunomodulatory properties in a mouse model of asthma that was dependent on regulatory T cells and tolerogenic dendritic cells (DC) (22). A related protein termed *Ac*-AIP-1 was recently shown to protect against inducible colitis by inducing accumulation of regulatory T cells in the mucosa and production of suppressor cytokines including IL-10 and TGF-β (23). Despite progress on the immunoregulatory properties of hookworm ES proteins, much less is known about the composition and anti-inflammatory properties of non-protein small metabolites or low molecular weight metabolites (LMWM; <10 kDa) in hookworm ESP (24).

Other nematodes, namely the parasitic *Ascaris lumbricoides* and free-living *Caenorhabditis elegans*, produce many biologically active LMWM including ascarosides and short chain fatty acids (SCFA) that have diverse biological properties (25). We therefore hypothesized that parasitic nematodes such as hookworms produce LMWM, some of which might have immunoregulatory properties and therefore present as potential anti-inflammatory drug candidates. Using the TNBS model of colitis, we demonstrate that select crude hookworm LMWM extracts afford significant protection against inducible acute colitis in mice and suppress *ex vivo* inflammatory cytokine production from human peripheral blood mononuclear cells (PBMC). Furthermore, we have undertaken both gas chromatography mass spectrometry (GC-MS)- and liquid chromatography mass spectrometry (LC-MS)-guided metabolomics analyses of *A. caninum* total somatic tissue extract and the anti-colitic fractions, and mined these datasets for likely anti-inflammatory candidates.

RESULTS

To understand the anti-inflammatory role of somatic tissue extracts of adult *A. caninum* and to identify small molecules present in the bioactive extracts, we collected hookworms from dogs, ground them into powder, extracted the LMWM with solvents, and then identified the LMWM present in these extracts using metabolomics techniques. The solvent extractions and preparation of crude extracts were conducted using natural products extraction protocols by sequentially extracting the ground powder with different solvents including mixed solvents of hexane: dichloromethane: acetronitrile (1:1:1 v/v; HDA), followed by dichloromethane (DCM), methanol (MeOH), acidified aqueous (Acidic) and basified aqueous (Basic) solvents. This extraction yielded five somatic extracts (SE) including SE-HDA, SE-DCM, SE-MeOH, SE-Acidic and SE-Basic, which were tested for their anti-inflammatory activities in a mouse model of TNBS-induced colitis and mitogen-stimulated human PBMC.

Hookworm SE-HDA and SE-MeOH protect mice against clinical symptoms of colitis. Five hookworm somatic tissue extracts were tested for their anti-inflammatory activities using the modified experimental design and TNBS induction in BALB/c mice as previously described by us (26). Extracts (50 μg/mouse) were administered intraperitoneally (i.p.) prior to intra-rectal (i.r.) injection of TNBS and the mice were monitored daily for three days for progression of clinical symptoms of colitis. Of five extracts tested, SE-HDA and SE-MeOH significantly protected mice against TNBS-induced clinical symptoms of colitis including body weight loss, lethargy (mobility), piloerection, diarrhea (fecal consistency) and fecal pellet counts (Fig.1).

<<<Insert Figure 1>>>

Mice treated with hookworm SE-HDA and SE-MeOH extracts showed reduced pathology. Mice were euthanized on the fifth day of the experiment and scored for pathological progression of colonic inflammation, and colon length was measured. In congruence with the clinical scores, colons of mice treated with SE-HDA and SE-MeOH showed significantly less colonic pathology than those of untreated mice, with significantly longer colon lengths (Fig. 2A), significantly reduced colon thickening (Fig. 2B), fewer adhesions (Fig. 2C), less edema (Fig. 2D), and less ulceration (Fig. 2E).

<<<Insert Figure 2>>>

Mice treated with hookworm SE-HDA and SE-MeOH showed well-preserved colon architecture. Of five hookworm extracts tested, SE-HDA and SE-MeOH showed well-preserved colon architecture in comparison to the TNBS control group (Fig.3). Naive (healthy control group) mice showed normal colon tissue architecture with healthy crypts and goblet cells, and normal lamina propria and mucosal integrity. Mice that were administered TNBS only (not treated with extracts) developed colitis and exhibited severe thickening of the lamina propria and colon wall musculature, edema, mucosal erosion and destruction of goblet cells. Increased numbers of leukocytes and polymorphonuclear cell infiltrates were clearly evident in the lamina propria and intraepithelial compartments of colons from untreated mice administered TNBS. Treatment with SE-HDA and SE-MeOH prior to administration of TNBS significantly protected against TNBS-induced histopathological damage. Treated mice had well-formed crypts, large numbers of goblet cells, and displayed generally healthy mucosal integrity that was comparable to naive mice that did not received TNBS. The other three hookworm LMWM extracts including SE-DCM, SE-Acidic and SE-Basic did not protect mice against histopathological damage induced by TNBS. Scoring of histological sections for overall colon pathology showed that mice

150 treated with SE-HDA extract had significantly reduced histopathology whereas the SE-MeOH-
151 treated group demonstrated a non-significant trend towards reduced histopathology when
152 compared with TNBS control mice.
153
154 <<<Insert Figure 3>>>
155 **Mice treated with hookworm SE-HDA and SE-MeOH extracts had non-significant**
156 **reductions in colonic inflammatory cytokine production.** Mouse colons were surgically
157 removed, cleaned of feces, sliced into 1 cm long pieces, cultured overnight and the supernatants
158 were assessed for colonic cytokine secretion levels. The protection of mice against clinical and
159 pathological changes was consistent with colonic cytokine responses, which showed a non-
160 significant trend towards reduced IFN-γ ($P = 0.3538$) and IL-17A ($P = 0.1510$) levels in mice
161 treated with SE-HDA and SE-MeOH (Fig.4).
162
163 <<<Insert Figure 4>>>
164
165 **SE-HDA suppressed *ex vivo* inflammatory cytokine production by human peripheral**
166 **blood mononuclear cells.** SE-HDA, SE-DCM and SE-MeOH were assessed for anti-
167 inflammatory properties on human PBMC stimulated *ex vivo* with lipopolysaccharide (LPS) to
168 promote cytokine production by myeloid cells or PMA/ionomycin to promote cytokine
169 production by T cells. T cell cytokine production was moderately reduced by SE-HDA at 20
170 μg/ml including a 14% reduction in IL-2 ($P < 0.001$), a 34% reduction in IL-6 ($P < 0.05$), a 59%
171 reduction in monocyte chemoattactant protein-1 (MCP-1) ($P < 0.001$) and a 33% reduction in
172 TNF-α ($P < 0.05$) (data not shown) compared to stimulated cells that were not co-cultured with
173 hookworm extracts. We observed a very potent effect of SE-HDA on myeloid cells. LPS-induced

cytokines were reduced in the presence of SE-HDA (at 20 μg/ml) including an 88% reduction in IL-1β ($P < 0.0001$), a 37% reduction in IL-6 ($P < 0.01$), a 58% reduction in TNF-α ($P < 0.01$) and an 84% reduction in MCP-1 ($P < 0.0001$) (Fig. 5).

<<<Insert Figure 5>>>

A dose-response analysis of the SE-HDA extract at final concentrations of 2, 10, 20 and 50 μg/ml showed that this extract significantly reduced the production of TNF-α, IL-1β, IL-6 and MCP-1 production by LPS-activated PBMC in a dose dependent manner (Fig. 6). The greatest suppression of cytokine secretion was observed for MCP-1, with SE-HDA concentrations as low as 2 μg/ml yielding significantly reduced chemokine secretion. At 50 μg/ml SE-HDA concentration, LPS-stimulated MCP-1 levels were the same as those of unstimulated PBMCs. Analysis of six genetically unrelated individuals showed that SE-HDA suppression of LPS-activated PBMC was consistent with significant reductions in IL-1β, IL-6, IL-12 and MCP-1. A paired analysis of supression in IL-1β and MCP-1 is shown in Fig. 6.

<<<Insert Figure 6>>>

SE-HDA and SE-MeOH somatic tissue extracts contain anti-inflammatory small metabolites. To characterize the small metabolites present in the protective somatic tissue extracts of *A. caninum*, we conducted targeted GC-MS and LC-MS metabolomics analyses of the underivatized SE-MeOH and SE-HDA extracts using methods described previously (27). The compounds were identified by comparing their ion patterns with the ion spectra of the known compounds indexed in the NIST database (28). Through GC-MS analyses, we identified a total of

198 32 metabolites from these two bioactive somatic tissue extracts (Table S1). Each extract
199 contained 20 metabolites, with 12 of them found exclusively in each extract. Both extracts
200 contained eight medium to long chain free saturated and unsaturated fatty acids (C_{11} to C_{26}).
201 Palmitic acid, methyl palmitate, stearic acid and methyl stearate were abundant in both extracts.
202 The most common mono/poly-unsaturated fatty acids present in both crude extracts were oleic
203 acid, linoleic acid, γ-linolenic acid and palmitoleic acid. Six of these fatty acids including stearic
204 acid (C18:0) (29), palmitic acid (C16:0) (30), methyl palmitate (31), γ-linolenic acid (32),
205 palmitoleic acid (C16:1n-7) (33) and oleic acid (C18:1) (29, 34) have been reported to exhibit
206 anti-inflammatory properties.

207 Using LC-MS, we identified eight SCFA, with isovalarate as the major component present
208 in both the SE-MeOH and SE-HDA somatic extracts. Acetate, propionate, butyrate, 2-
209 methylbutyrate, isovalerate, caproate and heptanoic acid were present in both protective
210 fractions/extracts (Table S2). Isobutyrate was present only in the SE-MeOH extract. Acetate,
211 propionate and butyrate (obtained from other synthetic sources) were previously reported to have
212 anti-inflammatory activities (35).

213 **Global metabolomes of derivatized whole worm somatic tissue extract of hookworms.**
214 Metabolomics analyses of two protective extracts **(**SE-HDA and SE-MeOH) showed only the
215 representative metabolomes of underivatized samples of hookworm extracts. To gain a global
216 insight of small metabolites present in *A. caninum*, we conducted a targeted GC-MS and LC-MS
217 metabolomics analyses of the methoximated, trimethylsilyl derivatized whole worm extract.
218 Whole worm extracts were divided into polar and non-polar fractions. From the polar fraction,
219 using GC-MS we identified 47 polar small metabolites (Table S3) belonging to seven
220 chemotypes including amino acids, sugars, sugar phosphates, organic acids, glycerides,
221 carbamides and oligosaccharides. Glycine, L-valine, L-proline, pyroglutamic acid, L-isoleucine,
222 L-tryptophan, D-talose, D-glucose, L-lysine and γ-aminobutyric acid (GABA) were present in

abundance. Eleven of these polar metabolites including glycine (36), L-isoleucine (37), L-lysine (38), γ-aminobutyric acid (GABA) (39), mannitol (40), D-ribose (41), trehalose (42), L-histidine (43), uridine (44), L-methionine (45) and citric acid (46) have been previously shown to exhibit anti-inflammatory activities against various diseases, including arthritis, renal inflammation, subarachnoid hemorrhage, pulmonary fibrosis and other conditions.

From the non-polar fraction, using GC-MS we identified 22 fatty acids (Table S4) comprising 17 saturated fatty acids (including stearic acid, palmitic acid, arachidic acid, margaric acid and myristic acid) and five unsaturated fatty acids (including elaidic acid, oleic acid, erucic acid, petroselinic acid, and nervonic acid). Literature review and content analyses revealed that at least seven of these fatty acids including stearic acid (C18:0) (29), palmitic acid (C16:0) (30), methyl palmitate (31), lauric acid (C12:0) (47), capric acid (C10:0) (47), γ-linolenic acid (32) and caprylic acid (C8:0) (48) were previously reported to have anti-inflammatory activities.

Using LC-MS analysis, we identified five SCFA from whole worm somatic tissue extracts, including isobutyrate, propionate, 2-methylvalerate, acetate and butyrate (Table S2). Of these SCFA, acetate (C2:0), propionate and butyrate (C4:0) have been reported to be effective in preventing inflammation associated with IBD (35).

DISCUSSION

Parasitic helminths, such as hookworms, have evolved to establish chronic infections in the human gut while inducing minimal pathology when present in low numbers (17). Hookworms regulate the immune system of the host for their benefit and subsequently promote a state of immune tolerance. This regulated environment not only promotes longevity for the parasites but also reduces the likelihood of the host developing diseases that result from a dysregulated immune system (49). A significant number of experimental and clinical studies support the immunoregulatory proficiency of parasitic helminths against distinct immunopathologies,

including allergies, IBD and other autoimmune diseases (9, 16, 50-53). While iatrogenic infection with hookworms and other helminths shows promise for treating numerous inflammatory diseases in humans, the therapy presents many challenges including patient apprehension, safety concerns and regulatory hurdles (17, 54). We and others showed that *A. caninum* ES proteins (>10 kDa) have potent immunomodulatory properties and can protect mice against pathology in different inducible models of colitis (17, 19, 20, 55, 56) and asthma (22). Non-proteinaceous small metabolites derived from helminths, however, have received far less attention in terms of their molecular characterization and their immunoregulatory properties. Indeed, we recently proposed that helminth LMWM warrant in-depth investigation as an untapped source of new drugs for treating inflammation (24). Here we provide a molecular characterization of hookworm LMWM and assess the efficacy of five different LMWM extracts in preventing both the onset of inducible colitis in mice and inflammatory cytokine production by primary human leukocytes.

Considering the relative strengths and limitations of all the available animal models, we chose the TNBS colitis model, which represents an intestinal immune response to environmental triggers, to investigate the anti-inflammatory properties of hookworm somatic LMWM. The TNBS model induces a mixed Th1/Th2/Th17 response (8), facilitating its use in screening for drugs targeting a broad range of inflammatory pathways. The intestinal mucosa of a TNBS-treated mouse is characterized by rapid production of inflammatory cytokines such as IFNγ and IL-17A (52). These cytokines are particularly important because disruption of the colonic mucosal layer by ethanolated TNBS dysregulates intestinal goblet cell function and elicits inflammation that drives the production of these cytokines. The colon contains epithelial goblet cells, which are instrumental in controlling intestinal immune homeostasis by producing a protective mucus layer. Therefore, any extracts/small molecules from intestinal worms that can promote retention of colonic mucus and inhibit inflammatory cytokine production have therapeutic potential. We showed that mice treated with *A. caninum* LMWM extracts (SE-MeOH

and SE-HDA) promoted retention of healthy gastrointestinal architecture after TNBS administration; this took the form of normal mucosal crypts, large numbers of unaltered goblet cells, and normal lamina propria and colon wall architecture in comparison to untreated groups that received TNBS. The colon culture supernatants and homogenates of these two treatment groups showed trends towards reduced expression (albeit non-significant) of TNBS-induced inflammatory cytokines, including IFN-γ and IL-17A. The protection conferred by SE-MeOH and SE-HDA extracts against TNBS-induced colitis was, however, more evident in their ability to significantly reduce body weight loss, improve clinical IBD related symptoms (including abridged mobility, piloerection and fecal consistency), and arrest pathological progression (including colon length shortening, colon wall thickening, adhesion, edema and ulceration). However, when these two anti-colitic somatic tissue extracts were assessed *ex vivo* for suppression of LPS-activated human PBMC, only treatment with SE-HDA resulted in significant suppression of pro-inflammatory cytokines including TNF-α, IL-1β, IL-6 and the chemokine MCP-1. Despite conferring robust protection against TNBS-induced colitis in mice, SE-MeOH did not suppress the production of LPS-stimulated cytokines by human PBMC. This could be due to distinct mechanisms of action of the bioactive components in each of the two models, or might also reflect the presence of different bioactive metabolites in the two distinct fractions. SE-HDA-induced suppression of inflammatory cytokines and chemokines was dose dependent, and particularly potent for MCP-1. MCP-1 and other chemotactic cytokines such as IL-8 induce chemotaxis, leukocyte activation and granule exocytosis, all of which increase chronic inflammation and intestinal tissue destruction in IBD (57).

The GC-MS and LC-MS analyses of these two anti-colitic somatic extracts (SE-MeOH and SE-HDA) revealed the presence of 32 small metabolites including eight medium-long chain fatty acids and seven SCFA. Some SM detected here such as ficusin, naphthalene derivative, methyl behenate and hentriacontanes are compounds known only from plants, and they are unlikely to be

298 synthesized by nematodes. Their putative appearance in these two helminths suggest the dietary
299 exposure of the host animals from which the hookworms were obtained. These SM are tentative
300 assignments pending MS-MS/NMR confirmation of proposed structures. From the whole worm
301 somatic tissue extract of *A. caninum*, we identified 47 polar metabolites (glycine as the major
302 amino acid), 22 fatty acids (stearic acid and methyl palmitate as major components) and four
303 SCFA (isovalerate as the major SCFA). The presence of a large number of polar metabolites was
304 consistent with the known dependence of these parasites on glucose metabolism, glycogen
305 synthesis, oxidative metabolism and phosphorylation (58-62). Palmitic acid and stearic acid were
306 the most common saturated fatty acids present in all the hookworm extracts. Palmitic acid is the
307 primary fatty acid from which other longer fatty acids are synthesized. Linoleic acid is found
308 mostly in plant glycosides and is used by animals in the biosynthesis of prostaglandins (via
309 arachidonic acid) and cell membranes (63). SCFA, including acetic, propionic, methylbutyric, *n*-
310 valeric and methylvaleric acids, were first reported in 1965 (64) from the cuticle, muscle and
311 reproductive systems of *A. lumbricoides*. Our findings concur with previous findings (62) on the
312 presence of SCFA in the ES products of *A. caninum*, where volatile SCFA such as acetic,
313 propionic, isobutyric and branched chain C_5 acids were detected (62). More recently, saturated
314 fatty acids were reported from the ova of *A. caninum* (65), but the authors did not report the
315 presence of SCFA.

316 The nature and origin of these excreted SCFA of *A. caninum* were demonstrated through
317 carbon (D-glucose-^{14}C) isotope/radiocarbon labeling, and indicated the presence of a glucose
318 metabolism intermediate between that observed in aerobes and that characteristic of helminth
319 anaerobes (62). The importance of SCFA as intermediates in the energy metabolism of intestinal
320 parasites in a succinate decarboxylase-dependent manner, as well as uncoupled mitochondrial
321 respiration, has been reported (66). A recent review (67) suggested that formation and excretion
322 of acetate as a metabolic end product of energy metabolism occurs in many protist (*Giardia*

323 *lamblia*, *Entamoeba histolytica*, *Trichomonas vaginalis*, *Trypanosoma* and *Leishmania* spp.) and
324 helminth (*Fasciola hepatica*, *Haemonchus contortus* and *Ascaris suum*) parasites from acetyl-
325 CoA by two different reactions, both involving substrate level phosphorylation that is catalyzed
326 by either a cytosolic acetyl-CoA synthetase or an organellar acetate:succinate CoA-transferase.
327 However, these enzymes involved in SCFA biosynthesis were poorly represented when we
328 mapped them against the known metabolic pathways (KEGG) of 81 worm genomes including the
329 human hookworm, *Necator americanus*, and the model free-living nematode, *C. elegans*. None of
330 the hookworm species represented in genome databases have any annotation associated with
331 SCFA synthesis other than two enzymes involved in propanoate synthesis. It is known that
332 parasitic helminths modulate intestinal inflammation *via* alteration of the composition of the gut
333 microbiota. This mechanism has been demonstrated both in rodent models (68) and human
334 studies where iatrogenic hookworm infection resulted in increased bacterial species richness and
335 elevated production of SCFA (11, 69). It is apparent that the gut microbiome is a complex
336 ecosystem with microbial syntrophy at the intestinal mucosal interface (70), and that SCFA such
337 as acetate, butyrate and propionate are produced and utilized by bacteria, and benefit host
338 epithelial cells by producing molecules like vitamin B_{12} (71). SCFA are key metabolites and
339 energy sources for commensal bacteria at the gut interface. Therefore, while it is possible that *A.*
340 *caninum* synthesizes SCFA *de novo*, further studies will be needed to define the contribution of
341 the commensal microbiome to SCFA synthesis in hookworms.

342 Analyses of the available literature on the biological activities of all the small molecules
343 identified from the somatic tissue extracts of *A. caninum* showed that 11 polar metabolites (36-
344 46), nine medium-long chain fatty acids (29-34, 47, 48), and three SCFA (35) have been
345 previously isolated from different sources and have been found to exhibit anti-inflammatory
346 activities. Of 23 anti-inflammatory small metabolites, only three compounds including one polar
347 metabolite (glycine) and three SCFA (acetate, propionate and butyrate) were studied *in vivo*

against chemically- and stress-induced ulcers in the gastric mucosa (36). Fatty acids, especially SCFA, have roles in host defense against potential opportunistic or pathogenic microorganisms, and establish an immunoregulatory environment that protects against inflammation in both the gastrointestinal tract and distant sites including the lung and heart (68, 72-74). SCFA are particularly important for colon homeostasis (72). For example, butyrate nourishes the colonic mucosa, and butyrate administration confers beneficial effects against IBD (72, 75). A comparative *in vitro* study of acetate (C2:0), propionate and butyrate (C4:0) revealed that propionate and butyrate were equipotent, where as acetate was less effective against IBD (35). Butyrate and propionate have also been implicated in the maintenance of host immune function by signaling to epithelial cells, maintaining regulatory T cell populations and inhibiting macrophage activation (70, 71). It is possible that *A. caninum* may be actively skewing the microbiome towards an anti-inflammatory composition by enhancing tolerogenic immune crosstalk through SCFA production. Chronic infection with *H. polygyrus* altered the intestinal habitat, resulting in increased SCFA production that was transferrable via the microbiota alone, and was sufficient to mediate protection against allergic asthma (68). The resulting anti-inflammatory cytokine secretion and regulatory T cell suppressor activity required the G protein-coupled receptor (GPR)-41, further highlighting the essential role of SCFA produced by commensal microbe communities shaped by the presence of helminth infections.

In summary, this study demonstrates that the somatic LMWM extracts of *A. caninum* are diverse in nature and possess anti-inflammatory properties that can suppress colitis in mice and inflammatory cytokine production by human leukocytes. Of five extracts tested, SE-MeOH and SE-HDA significantly protected mice against chemically-induced colitis, which implied that methanol and HDA were the best solvents to extract bioactive metabolites from hookworm somatic tissues. Our GC-MS and LC-MS analyses highlighted the presence of multiple small molecules in these fractions. Several of these metabolites, including the SCFA, have been

373 previously shown to have anti-inflammatory properties in various target diseases, including IBD.
374 It is possible that these anti-inflammatory small molecules, either individually or in synergy, are
375 responsible for the anti-inflammatory properties of SE-MeOH and SE-HDA extracts of *A.*
376 *caninum.* Future work will entail purification and isolation of the bioactive metabolites, synthesis
377 of the candidate components, and detailed pharmacotherapeutic assessment of the anti-colitic
378 properties of the candidate compounds using a chronic immunologic mouse model of colitis.
379 Moreover, while it is difficult to obtain large quantities of hookworm ESP, efforts should be
380 invested in further isolating the ESP metabolomes with a focus on understanding the source and
381 nature of SCFA, given that these compounds have specifically evolved to interact with host
382 tissues and play important roles in regulating inflammation.
383
384 ## MATERIALS AND METHODS

385 **Hookworm collection.** *A. caninum* adult worms were collected with clockmaker tweezers
386 from the small intestine of infected dogs and transferred to pre-warmed culture media (2%
387 Glutamax in phosphate buffered saline (PBS), 5% antibiotic/antimycotic [AA]) in 50 ml falcon
388 tubes. *A. caninum* adult worms were thoroughly washed with 5× antimycotic/antibiotic solution
389 to purge bacterial contaminants and were cultured (50 worms per dish) in a single component
390 Glutamax medium (2% Glutamax in PBS supplemented with 2× AA) for 2 h at 37°C in 5% CO_2
391 to allow regurgitation/defecation of the host blood meal and other material (including bacteria)
392 that may have been acquired from the dog host gut. The worms were then snap-frozen in liquid
393 nitrogen until further use.

394 **Preparation of hookworm somatic extracts.** The adult worms were frozen with liquid
395 nitrogen and made into powder using a mortar and pestle. The powder was first soaked in a
396 solvent mixture of hexane:dichloromethane:acetonitrile (1:1:1 v/v, 6 ml/g; HDA) for 30 min and

was filtered (Whatman 4, Qualitative circles 185 mm, England International Ltd.). The extraction of cell material on filter paper was repeated three times with the same solvent. The filtrates were combined, centrifuged at 1,831 *g* (Rotina 420 R, Hettich Zentrifugen, Germany) for 20 minutes at 4°C and the supernatant slowly transferred to round-bottom flasks. The solvent was removed using a Rotary Evaporator (G5 Heidolf CVC 3000 Vacuubrand) to obtain the somatic tissue HDA fraction (SE-HDA). The solid residue was snap-frozen in liquid nitrogen, powdered and extracted with dichloromethane (3×). The filtration, centrifugation and drying processes were repeated as above to obtain the DCM fraction (SE-DCM). The remaining somatic tissue was snap-frozen again, powdered and extracted with methanol to obtain the MeOH fraction (SE-MeOH). Remaining solid residue from this step was snap frozen and soaked in 5% HCL (pH 1-2). The supernatant was freeze-dried using a Scanvac Cool Safe to obtain acidified aqueous extract (SE-Acidic). The solid tissues were finally soaked in basified (NH_4OH, pH 10-12) water, filtered and centrifuged at 1,831 *g*, and freeze-dried to obtain alkaline aqueous extract (SE-Basic). Stock concentrations of these extracts (1 mg/ml) were prepared by dissolving 1 mg of each extract in 20 µL of DMSO followed by addition of 980 µl of PBS. From each stock concentration, 50 µl was transferred to a vial and added to 150 µl of fresh PBS to make a total injectable volume of 200 µl/mouse. These extracts were assessed for efficacy in the TNBS model of acute colitis.

Animal ethics, source and housing of mice. The James Cook University (JCU) animal ethics committee approved all experimental work involving animals (Ethics approval number A2199). Mice were raised in cages in the JCU animal facility in compliance with the Australian Code of Practice for the Care and Use of Animals for Scientific Purposes, 7th edition, 2007 and the Queensland Animal Care and Protection Act 2001. Age-matched 5-week old male BALB/c mice were sourced from Animal Resources Centre (Perth, Australia), weighed, placed in cages (5 mice per cage), and allowed to settle into the study facility for 4-5 days prior to the start of the

422 experiment. Animals were housed in a temperature (26°C) and humidity-controlled (40-70%)
423 environment, exposed to a 12-hour day/night cycle, and provided with irradiated mouse chow
424 supplied by Specialty Feeds (Glen Forrest, Western Australia) and autoclaved tap water *ad*
425 *libitum*.

426 **Experimental design and induction of TNBS colitis**. We followed the modified
427 experimental design and TNBS induction protocols described by us earlier (26). Mice were
428 divided into three different groups as "Naïve", "TNBS only" and "TNBS + Sample treatment".
429 This experiment was performed in duplicate (total n=10 mice/group). The samples were filtered
430 using 0.22 µM sterile filters prior to intra-peritoneal (i.p) administration to mice. Each mouse in
431 the "Sample treatment" groups (each group labelled as SE-HDA, SE-DCM, SE-MeOH, SE-
432 Acidic and SE-Basic) received 50 µl of extract suspension/mouse by i.p. injection (Day 1). The
433 TNBS only group was administered 200 µl of PBS/DMSO (1%). Twenty-four hours post sample
434 administration (Day 2), the mice were anaesthetized by i.p. injection of anesthetic solution
435 containing 50 mg/kg of ketamine and 5 mg/kg of xylazine. TNBS was administered by intra-
436 rectal (i.r.) injection of 100 µl TNBS (2.5 mg/mouse) mixed with 50% ethanol using a soft
437 catheter (Insyte Autoguard Shielded IV catheter 20G x 1" Pink; Becton Dickinson). Mice were
438 kept inverted for 2 minutes to prevent leakage of TNBS and returned to their cages. Mice were
439 monitored daily until euthanized at day 5.

440 **Monitoring colitis progression by clinical scoring.** Mice were clinically scored for
441 weight loss, piloerection, mobility, fecal consistency and fecal pellet counts for 3 days following
442 administration of TNBS. Each individual mouse was placed in a clean cage/open plastic jar and
443 observed for 10 minutes to score the clinical symptoms. The changes in clinical signs of disease
444 were scored from 0-2, 0 being normal and 2 being diseased. A score of "0" was given when the
445 mice gained weight, "1" when weight remained the same and "2" upon losing weight. Mice with
446 no piloerection scored "0," mild piloerection over the neck as "1" and severe piloerection all over

447 the body as "2". The mobility of a mouse was scored as "0" for normal, "1" for movement only
448 after stimulation, and "2" for hunched posture with no movement around the cage, even after
449 stimulation. For fecal consistency, normal feces were scored "0", mild diarrhea was scored "1"
450 and severe diarrhea with blood or no feces was scored "2". After 10 minutes of isolation, the
451 fecal pellets were counted (higher number of pellets indicated normal or mice recovering from
452 chemical colitis).

453 **Assessing intestinal pathology and macroscopic scoring.** On day 5 post-TNBS
454 administration, the mice were euthanized. Their colons (from cecum to rectum) were surgically
455 removed, measured and assessed for changes in macroscopic appearance and pathological
456 parameters including adhesions, bowel wall thickening and edema (scoring matrices of 0–3; 0 =
457 normal, 1 = mild, 2 = moderate, and 3 = severe). The colons from each group were lined up on a
458 clean surgical drape paper towel, their lengths measured and then transferred to a petri dish in
459 sterile DPBS. The tissues were opened longitudinally, washed with DPBS, placed under a
460 microscope (Olympus SZ61, 0.67–4.5×), observed for inflamed sections, and scored for
461 ulceration (0 – 3).

462 **Evaluating colon histological structure.** The distal colon tissue sections (1 cm) that
463 were harvested from mice were placed in 4% paraformaldehyde (1 ml) to fix tissue overnight at
464 4°C and then transferred to 70% ethanol for storage. Tissue was embedded in paraffin and
465 sectioned longitudinally for histology at 4 μm thickness. Sections were stained with hematoxylin
466 and eosin (H/E), observed for histological changes by light microscopy and histological
467 photomicrographs (×200) were captured. Each histological photomicrograph was blinded and
468 then scored for changes in overall colon morphology and epithelial integrity. The cross-sections
469 of the colon tissues were scored for inflammation, edema, hyperplasia, ulceration and number of
470 goblets cells using a scoring matrix (76). An AxioCam Imager –M1 (MRC ZEISS) was used for

scoring the colon histology cross-sections.

ELISAs and cytokine measurement of colon tissues. Colon pieces (1 cm) were collected and placed in sterile 24 well tissue culture plates with 500 µl of complete medium (RPMI containing 10% fetal bovine serum, 1% penicillin/streptomycin, 0.1% β-mercaptoethanol, 1% HEPES buffer. Tissues were cultured for 24 h at 37°C (supplied with 5% CO_2) after which supernatants were collected and stored at −80°C until further analysis. Colon culture supernatants were thawed and levels of cytokines were quantified using a sandwich enzyme-linked immunosorbent assay (ELISA) (Ready-SET-Go!, eBiosciences) following the manufacturer's instructions. OD_{490} values were measured using a POLARstar Omega plate reader (BMG LABTECH) and were expressed as picogram (pg) of tissue weight per mL.

Human PBMC collection and culture conditions. The human blood used for this study was obtained from healthy volunteer donors. Written informed consent was obtained from each donor at the time of blood draw. Ethical approval for this research was obtained from the James Cook University Human Ethics Committee. PBMC were isolated from whole blood by density gradient centrifugation using Ficoll-Paque media. For induction of T cell cytokines, PBMC were activated with a cell stimulation cocktail of 50 ng/ml of phorbol 12- myristate 13-acetate (PMA) and 1 µg/ml of ionomycin (eBioscience). PMA + ionomycin-stimulated cells were treated with 20 µg/ml of hookworm extracts (SE-HDA, SE-DCM, SE-MeOH) or remained untreated. For stimulation of myeloid-associated cytokines, PBMC were activated with 10 ng/ml lipopolysaccharide (LPS) (Sigma-Aldrich). LPS-stimulated PBMC were treated with 2-50 µg/ml of hookworm extracts (SE-HDA, SE-DCM, SE-MeOH) or remained untreated. The cell culture plates were incubated overnight at 37°C and 6.5% CO_2. After incubation, the samples were centrifuged at 1,500 *g* for 5 minutes and the culture supernatants were collected for cytokine analysis.

BD™ Cytometric Bead Array. IL-1β, IL-6, IL-12, TNF-α and MCP-1 from PBMC culture supernatant were quantified using a cytometric bead array (CBA) (BD™ Biosciences). The CBA assays were performed according to the manufacturer's instruction and run using a five laser Special Order LSRFortessa™ with HTS (BD Biosciences). Cytokine concentrations (pg/ml) were calculated based on the sample MFI compared to the cytokine standard curves. BD™ FCAP Array software version 3.0 was used for data analysis. Graphs and statistical analysis were produced using GraphPad Prism version 7.02 (GraphPad Software Inc).

Cryomill somatic tissue extraction of adult worms for GC-MS metabolomics analysis. Somatic tissue extract of adult *A. caninum* (10-20 mg) was snap-frozen in liquid nitrogen to arrest metabolic changes, placed in cryomill tubes, then suspended in 600 µl extraction solution (methanol:water 3:1 (v/v) containing internal standards ^{13}C,^{15}N-valine and ^{13}C-sorbitol). The sample was extracted using a Precellys 24 Cryolys unit (Bertin Technologies) at 6800 rpm, 3 × 30 sec pulses, 45 second interval between pulses, temperature < –5°C (pre-chilled with liquid nitrogen). The homogenate was transferred to a fresh microfuge tube on ice and chilled chloroform (150 µl) was added. The solution (chloroform:methanol:water 1:3:1 (v/v) monophasic mixture) was vortexed vigorously chilled on ice for 10 minutes with regular mixing and then centrifuged for 5 minutes at 0°C. The supernatant was transferred to a fresh 1.5 ml microfuge tube on ice and milli-Q water (300 µL) was added to each tube to obtain a biphasic partition of the solution (chloroform:methanol:water 1:3:3 (v/v)). The sample was vortexed vigorously and then centrifuged at 0°C for a further 5 minutes.

For total fatty acid analyses, the bottom chloroform extract (45 µl) was transferred to fresh tubes and 0.2M *m*-trifluromethylphenyl trimethyl ammonium hydroxide (methprep) (5 µl) was added. Samples (5 replicates) were mixed using a thermomixer at 750 rpm for 30 minutes at 37°C. The samples were injected (2 µl) into an Agilent 7000 triple quad GC-MS (1:10 split

injection, BPX70 60 m x 0.25 mm x 0.25 µm column) and the raw data were obtained and processed.

Derivatization method for targeted metabolite analysis using GC-MS. The upper aqueous phase (methanol:water, ~900 µl) was transferred to a fresh tube, then aliquoted (50 µl) into a pulled point insert and dried in an evaporator (Christ RVC 2-33 CD, John Morris Scientific Australia) at 35°C. A further 50 µl of the aqueous sample was added every 30-40 minutes until completely dry. Samples were dehydrated by adding 50 µl anhydrous methanol, and then derivatized by addition of 20 µl methoxyamine (30 mg/ml in pyridine, Sigma Aldrich/Merck) at 37°C for 30 minutes, and then 20 µl of *N,O*-Bis(trimethylsilyl) trifluoroacetamide (BSTFA) + 1% trimethylchlorosilane (TMCS) (ThermoFisher Scientific) was added prior to incubation at 37°C for 30 minutes. The derivatized sample (1 µl) was analyzed using an Agilent 7890 GC-MS (5973 MSD) (77). Chromatographic separation was achieved using an Agilent VF-5 ms column (30 m × 0.25 mm × 0.25 µm). Conditions for the oven were set at 35°C, held for 2 minutes, then ramped at 25°C/minute to 325°C and held for 5 minutes. Helium was used as the carrier gas at a flow rate of 1 ml/minute, with compounds being detected across the m/z range of 50–600 atomic mass unit (amu).

GC-MS analyses of SE-HDA and SE-MeOH extracts using underivatized protocols. We performed GC-MS analysis on the two bioactive extracts using methods described by us previously (78). The dried crude fractions were re-suspended in chloroform-methanol solvent (90%:10%) and were directly injected into a Shimadzu GC-2010 Plus system to analyse their chemical constituents. The GC system used helium as a carrier gas (1.22 mL/min, pressure 67.7 kPa at 40°C in a constant total flow mode) and the separation was achieved using a DB-5 ms column (l30 m length × 0.25 mm, i.d., 0.25 µm, Phenomenex). Injector (injection – splitless mode) and detector temperatures were set at 225°C and 300°C, respectively. The starting oven temperature was programmed at 45°C with an increasing temperature of 3°C/minute until it

reached 100°C (hold time = 4 minutes) and final temperature of 240°C (hold time = 50 minutes). Similarly, the same equipment was programed for the MS system (condition and column same as above) with a runtime of 90 minutes (ion source = 200°C, solvent cut time = 1 minute, threshold = 0, starting mass (*m/z*) = 35 and maximum mass measured (*m/z*) = 1000, acquisition mode = scan, scan speed = 3333). The GC-MS was acquired in scan mode producing a total ion chromatogram (TIC).

The chemical constituents were identified by comparing and matching the ion fragmentation patterns of the test sample compounds with the National Institute of Standards and Technology (NIST, USA) mass spectra library of GC-MS data. Each compound was then surveyed for erstwhile literature on their anti-inflammatory properties using SciFinder Scholar, PubMed and Google Scholar. Published studies reporting anti-inflammatory activities for each compound are cited in the relevant tables.

Identification of SCFA using LC-MS protocols. The SCFA in the protective SE-HDA and SE-MeOH extracts, and the whole worm extract of hookworms were analysed by LC-MS in accordance with previously described protocols (79). Samples were analyzed in triplicate. Known SCFA, including acetate, propionate, isobutyrate, butyrate, 2-methylbutyrate, isovalerate, valerate, 3-NPH, 2-methylvalerate, 3-methylvalerate, isocaproate, caproate and heptanoic acid were used as standards (5 μM and 50 μM concentrations). These SCFA were mapped against the existing 81 worm genome KEGG pathways to understand their biosynthetic nature.

Statistical and data analyses. The data from groups of mice from 2 independent experiments (N =10) were combined and the statistical analyses were performed using GraphPad Prism (version 7.0) as described earlier (76). Comparisons were made between the sample treatment + TNBS groups and the TNBS only group; P values of < 0.05 were considered significant. When determining the differences between more than two groups with equal numbers of mice/samples, 2-way ANOVA was used. When two groups were compared a Mann-Whitney

(unpaired, non-parametric) t-test was applied. All results reported denote mean ± standard error of the mean (SEM). The metabolomics data was analyzed in a targeted approach using Agilent's Mass Hunter Quantitative Analysis software (v.7). Target ion peak areas for polar and non-polar metabolites were extracted using the in-house Metabolomics Australia metabolite library and were integrated and output as a data matrix for further analysis (section 3.5).

ACKNOWLEDGMENTS

This study was supported by a NHMRC Peter Doherty Early Career Researcher Fellowship (APP1091011) and AITHM Capacity Development Grant to P.W; a NHMRC program grant APP1037304 and NHMRC Senior Principal Research Fellowship (APP1117504) to A.L; and a NHMRC Career Development Fellowship (APP1131732) to J.J.M.

We thank Dr. Makedonka Mitreva for hookworm genome analyses, Dr. Severine Navarro, Mr. Atik Susianto, Dr. Komal Kanojia, Dr. Vinod Narayana and Mr. Bjoernar Hauge for assistance with cytokine analyses, SCFA method development for hookworm extracts and animal husbandry.

REFERENCES

1. Crohn's & Colitis Foundation of America. 2014. The facts about inflammatory bowel diseases. Crohn's & Colitis Foundation of America, New York.
2. Crohn's & Colitis Australia. 2014. Annual Report 2012-2013. Australia.
3. Ng CS. 2016. Emerging trends of inflammatory bowel disease in Asia. Gastroenterol Hepatol 12:193-196.
4. Jose FA, Heyman MB. 2008. Extraintestinal manifestations of inflammatory bowel disease. J Pediatr Gastroenterol Nutr 46:124-133.

5. Szigethy E. 2016. Gut feelings. Nature S113.

6. Niewiadomski O, Studd C, Hair C, Wilson J, Ding NS, Heerasing N, Ting A, McNeill J, Knight R, Santamaria J, Prewett E, Dabkowski P, Dowling D, Alexander S, Allen B, Popp B, Connell W, Desmond P, Bell S. 2015. Prospective population-based cohort of inflammatory bowel disease in the biologics era: Disease course and predictors of severity. J Gastroenterol Hepatol 30:1346-53.

7. Brown C, Gibson PR, Hart A, Kaplan GG, Kachroo S, Ding Q, Hautamaki E, Fan T, Black CM, Hu X, Beusterien K. 2015. Long-term outcomes of colectomy surgery among patients with ulcerative colitis. Springerplus 4:573.

8. Neurath MF. 2017. Current and emerging therapeutic targets for IBD. Nat Rev Gastroenterol Hepatol 14:688.

9. Daveson J, Jones DM, Gaze S, McSorley H, Clouston A, Pascoe A, Cooke S, Speare R, Macdonald GA, Anderson R, McCarthy JS, Loukas A, Croese J. 2011. Effect of hookworm infection on wheat challenge in celiac disease-a randomised double-blinded placebo controlled trial. PLoS One 6:e17366.

10. Gaze S, McSorley HJ, Daveson J, Jones D, Bethony JM, Oliveira LM, Speare R, McCarthy JS, Engwerda CR, Croese J, Loukas A. 2012. Characterising the mucosal and systemic immune responses to experimental human hookworm infection. PLoS Pathog 8:e1002520.

11. Giacomin P, Zakrzewski M, Croese J, Su X, Sotillo J, McCann L, Navarro S, Mitreva M, Krause L, Loukas A, Cantacessi C. 2015. Experimental hookworm infection and escalating gluten challenges are associated with increased microbial richness in celiac subjects. Sci Rep 18:13797.

12. McSorley HJ, Gaze S, Daveson J, Jones D, Anderson RP, Clouston A, Ruyssers NE, Speare R, McCarthy JS, Engwerda CR, Croese J, Loukas A. 2011. Suppression of

619 inflammatory immune responses in celiac disease by experimental hookworm infection.
620 PLoS One 6:e24092.
621 13. Smallwood TB, Giacomin PR, Loukas A, Mulvenna JP, Clark RJ, Miles JJ. 2017.
622 Helminth immunomodulation in autoimmune disease. Front Immunol 8:453.
623 14. Blount J, Hooi D, Feary J, Venn A, Telford G, Brown A, Britton J, Pritchard D. 2009.
624 Immunologic profiles of persons recruited for a randomized, placebo-controlled clinical
625 trial of hookworm infection. Am J Trop Med Hyg 81:911-916.
626 15. Geiger SM, Fujiwara RT, Santiago H, Corrêa-Oliveira R, Bethony JM. 2008. Early stage-
627 specific immune responses in primary experimental human hookworm infection.
628 Microbes Infect 10:1524-1535.
629 16. Croese J, O'neil J, Masson J, Cooke S, Melrose W, Pritchard D, Speare R. 2006. A proof
630 of concept study establishing *Necator americanus* in Crohn's patients and reservoir
631 donors. Gut 55:136-137.
632 17. Loukas A, Hotez PJ, Diemert D, Yazdanbakhsh M, McCarthy JS, Correa-Oliveira R,
633 Croese J, Bethony JM. 2016. Hookworm infection. Nat Rev Dis Primers 2:16088.
634 18. Yazdanbakhsh M, Kremsner PG, van Ree R. 2002. Allergy, parasites, and the hygiene
635 hypothesis. Science 296:490-494.
636 19. Ruyssers NE, De Winter BY, De Man JG, Loukas A, Pearson MS, Weinstock JV, Van
637 den Bossche RM, Martinet W, Pelckmans PA, Moreels TG. 2009. Therapeutic potential
638 of helminth soluble proteins in TNBS-induced colitis in mice. Inflamm Bowel Dis
639 15:491.
640 20. Ferreira I, Smyth D, Gaze S, Aziz A, Giacomin P, Ruyssers N, Artis D, Laha T, Navarro
641 S, Loukas A, McSorley HJ. 2013. Hookworm excretory/secretory products induce
642 interleukin-4 (IL-4)+ IL-10+ CD4+ T cell responses and suppress pathology in a mouse
643 model of colitis. Infect Immun 81:2104-2111.

644 21. Mulvenna J, Hamilton B, Nagaraj SH, Smyth D, Loukas A, Gorman JJ. 2009. Proteomics
645 analysis of the excretory/secretory component of the blood-feeding stage of the
646 hookworm, *Ancylostoma caninum*. Mol Cell Proteomics 8:109-21.
647 22. Navarro S, Pickering DA, Ferreira IB, Jones L, Ryan S, Troy S, Leech A, Hotez PJ, Zhan
648 B, Laha T, Prentice R, Sparwasser T, Croese J, Engwerda CR, Upham JW, Julia V,
649 Giacomin PR, Loukas A. 2016. Hookworm recombinant protein promotes regulatory T
650 cell responses that suppress experimental asthma. Sci Transl Med 8:362ra143.
651 23. Ferreira IB, Pickering DA, Troy S, Croese J, Loukas A, Navarro S. 2017. Suppression of
652 inflammation and tissue damage by a hookworm recombinant protein in experimental
653 colitis. Clin Transl Immunology 6:e157.
654 24. Shepherd C, Navarro S, Wangchuk P, Wilson D, Daly NL, Loukas A. 2015. Identifying
655 the immunomodulatory components of helminths. Parasite Immunol 37:293-303.
656 25. Kaplan F, Srinivasan J, Mahanti P, Ajredini R, Durak O, Nimalendran R, Sternberg PW,
657 Teal PE, Schroeder FC, Edison AS, Alborn HT. 2011. Ascaroside expression in
658 *Caenorhabditis elegans* is strongly dependent on diet and developmental stage. PLoS One
659 6:e17804.
660 26. Wangchuk P, Navarro S, Shepherd C, Keller PA, Pyne SG, Loukas A. 2015. Diterpenoid
661 alkaloids of *Aconitum laciniatum* and mitigation of inflammation by 14-*O*-acetylneoline
662 in a murine model of ulcerative colitis. Sci Rep 5:12845.
663 27. Wangchuk P, Samten. 2015. GC-FID coupled GC-MS analysis of the essential oil and the
664 recorded biological activities of *Meconopsis simplicifolia*. J Biologic Active Prod Nature
665 5:365-372.
666 28. Stein SE. 2014. NIST Standard Reference Database 1A v14 National Institute of
667 Standards and Technology, Gaithersburg.

668 29. Ahmad M, Baba WN, Gani A, Wani TA, Gani A, Masoodi FA. 2015. Effect of extraction
669 time on antioxidants and bioactive volatile components of green tea (*Camellia sinensis*),
670 using GC/MS. Cogent Food Agric 1:1106387.
671 30. Aparna V, Dileep KV, Mandal PK, Karthe P, Sadasivan C, Haridas M. 2012. Anti-
672 Inflammatory property of *n*-hexadecanoic acid: structural evidence and kinetic
673 assessment. Chem Biol Drug Des 80:434-439.
674 31. El-Demerdash E. 2011. Anti-inflammatory and antifibrotic effects of methyl palmitate.
675 Toxicol Appl Pharmacol 254:238-244.
676 32. Kim DH, Yoo TH, Lee SH, Kang HY, Nam BY, Kwak SJ, Kim JK, Park JT, Han SH,
677 Kang SW. 2012. Gamma linolenic acid exerts anti-inflammatory and anti-fibrotic effects
678 in diabetic nephropathy. Yonsei Med J 53:1165-1175.
679 33. Morse N. 2015. Lipid-lowering and anti-inflammatory effects of palmitoleic acid:
680 Evidence from preclinical and epidemiological studies. Lipid Technol 27:107-111.
681 34. Gopalakrishnan S, Vadivel E. 2011. GC-MS analysis of some bioactive constituents of
682 *Mussaenda frondosa* Linn. Int J Pharma Biosci 2:313-320.
683 35. Tedelind S, Westverg F, Kjerrulf M, Vidal A. 2007. Anti-inflammatory properties of the
684 short-chain fatty acids acetate and propionate: A study with relevance to inflammatory
685 bowel disease. World J Gastroenterol 13:2826-2832.
686 36. Zhong Z, Wheeler MD, Li X, Froh M, Schemmer P, Yin M, Bunzendaul H, Bradford B,
687 Lemasters JJ. 2003. L-Glycine: a novel antiinflammatory, immunomodulatory, and
688 cytoprotective agent. Curr Opin Clin Nutr Metab Care 6:229-40.
689 37. Saxena RN, Pendse VK, Khanna NK. 1984. Anti-inflammatory and analgesic properties
690 of four amino-acids. Indian J Physiol Pharmacol 28:299-305.

691 38. Mine Y, Zhang H. 2015. Anti-inflammatory effects of poly-L-lysine in intestinal mucosal
692 system mediated by calcium-sensing receptor activation. J Agric Food Chem 63:10437-
693 47.
694 39. Han D, Kim HY, Lee HJ, Shim I, Hahm DH. 2007. Wound healing activity of gamma-
695 aminobutyric acid (GABA) in rats. J Microbiol Biotechnol 17:1661-1669.
696 40. Cavone L, Calosi L, Cinci L, Moroni F, Chiarugi A. 2012. Topical mannitol reduces
697 inflammatory edema in a rat model of arthritis. Pharmacology 89:18-21.
698 41. Ueki M, Ueno M, Morishita J, Maekawa N. 2013. D-ribose ameliorates cisplatin-induced
699 nephrotoxicity by inhibiting renal inflammation in mice. Tohoku J Exp Med 229:195-201.
700 42. Echigo R, Shimohata N, Karatsu K, Yano F, Kayasuga-Kariya Y, Fujisawa A, Ohto T,
701 Kita Y, Nakamura M, Suzuki S, Mochizuki M, Shimizu T, Chung U, Sasaki N. 2012.
702 Trehalose treatment suppresses inflammation, oxidative stress, and vasospasm induced by
703 experimental subarachnoid hemorrhage. J Transl Med 10:80.
704 43. Hasegawa S, Ichiyama T, Sonaka I, Ohsaki A, Okada S, Wakiguchi H, Kudo K, Kittaka
705 S, Hara M, Furukawa S. 2012. Cysteine, histidine and glycine exhibit anti-inflammatory
706 effects in human coronary arterial endothelial cells. Clin Exp Immunol 167:269-274.
707 44. Cicko S, Grimm M, Ayata K, Beckert J, Meyer A, Hossfeld M, Zissel G, Idzko M, Müller
708 T. 2015. Uridine supplementation exerts anti-inflammatory and anti-fibrotic effects in an
709 animal model of pulmonary fibrosis. Respir Res 16:105.
710 45. Unnikrishnan MK, Rao MN. 1990. Antiinflammatory activity of methionine, methionine
711 sulfoxide and methionine sulfone. Agents Actions 31:110-2.
712 46. Abdel-Salam OM, Youness ER, Mohammed NA, Morsy SM, Omara EA, Sleem AA.
713 2014. Citric acid effects on brain and liver oxidative stress in lipopolysaccharide-treated
714 mice. J Med Food 17:588-598.

715 47. Huang WC, Tsai TH, Chuang LT, Li YY, Zouboulis CC, Tsai PJ. 2014. Antibacterial and
716 anti-inflammatory properties of capric acid against propionibacterium acnes: A
717 comparative study with lauric acid. J Dermatol Sci 73:232-240.
718 48. Hoshimoto A, Suzuki Y, Katsuno T, Nakajima H, Saito Y. 2002. Caprylic acid and
719 medium-chain triglycerides inhibit IL-8 gene transcription in Caco-2 cells: comparison
720 with the potent histone deacetylase inhibitor trichostatin A. Br J Pharmacol 136:280-286.
721 49. Varyani F, Fleming JO, Maizels RM. 2017. Helminths in the gastrointestinal tract as
722 modulators of immunity and pathology. Am J Physiol Gastrointest Liver Physiol
723 312:G537-G549.
724 50. Leung J, Hang L, Blum A, Setiawan T, Stoyanoff K, Weinstock J. 2012.
725 *Heligmosomoides polygyrus* abrogates antigen-specific gut injury in a murine model of
726 inflammatory bowel disease. Inflamm Bowel Dis 18:1447-1455.
727 51. Reardon C, Sanchez A, Hogaboam CM, McKay DM. 2001. Tapeworm infection reduces
728 epithelial ion transport abnormalities in murine dextran sulfate sodium-induced colitis.
729 Infect Immun 69:4417-4423.
730 52. Weinstock JV, Elliott DE. 2013. Translatability of helminth therapy in inflammatory
731 bowel diseases. Int J Parasitol 43:245-251.
732 53. Yang X, Yang Y, Wang Y, Zhan B, Gu Y, Cheng Y, Zhu X. 2014. Excretory/secretory
733 products from *Trichinella spiralis* adult worms ameliorate DSS-induced colitis in mice.
734 PLoS One 9:e96454.
735 54. Maizels RM. 2016. Parasitic helminth infections and the control of human allergic and
736 autoimmune disorders. Clin Microbiol Infect 22:481-6.
737 55. Ferreira IB, Pickering DA, Troy S, Croese J, Loukas A, Navarro S. 2017. Suppression of
738 inflammation and tissue damage by a hookworm recombinant protein in experimental
739 colitis. Clin Transl Immunology 6:e157.

740 56. Cançado GG, Fiuza JA, de Paiva NC, Lemos Lde C, Ricci ND, Gazzinelli-Guimarães PH,
741 Martins VG, Bartholomeu DC, Negrão-Corrêa DA, Carneiro CM, Fujiwara RT. 2011.
742 Hookworm products ameliorate dextran sodium sulfate-induced colitis in BALB/c mice.
743 Inflamm Bowel Dis 17:2275-86.
744 57. MacDermott RP, Sanderson IR, HC. R. 1998. The central role of chemokines
745 (chemotactic cytokines) in the immunopathogenesis of ulcerative colitis and Crohn's
746 disease. Inflamm Bowel Dis 4:54-67.
747 58. Fernando MA, Wong HA. 1964. Metabolism of hookworms. II. Glucose metabolism and
748 glycogen synthesis in adult femeale *Ancyclostoma caninum*. Exp Parasitol 15:284-292.
749 59. Warren LG, Karlsson EL. 1965. Biochemistry of the dog hookworm. I. Oxidative
750 metabolism. Exp Parasitol 17:1-19.
751 60. Warren LG. 1970. Biochemistry of the dog hookworm. III. Oxidative phosphorylation.
752 Exp Parasitol 27:417-423.
753 61. Gimenez ME, Gimenez A, Gaede K. 1967. Metabolic transformation of 14C-Glucose into
754 tissue proteins of *Ancyclostoma caninum*. Exp Parasitol 21:215-223.
755 62. Warren LG, Poole WJ. 1970. Biochemistry of the dog hookworm II. Nature and origin of
756 the excreted fatty acids. Exp Parasitol 27:408-416.
757 63. National Center for Biotechnology Information. Linoleic acid. PubChem Compound
758 Database; CID=5280450, https://pubchem.ncbi.nlm.nih.gov/compound/5280450
759 (accessed Apr. 16, 2018.
760 64. Beames CGJ. 1965. Neutral lipids of Ascaris lumbricoides with special reference to the
761 esterified fatty acids. Exp Parasitol 16:291-9.
762 65. Gyawali P, Beale DJ, Ahmed W, Karpe AV, Magalhaes RJ. 2016. Determination of
763 *Ancylostoma caninum* ova viability using metabolic profiling. Parasitol Res 115:3485-
764 3492.

765 66. Saz HJ. 1981. Energy metabolisms of parasitic helminths: adaptations to parasitism. Ann
766 Rev Physiol 43:323-341.
767 67. Tielens AGM, van Grinsven KWA, Henze K, van Hellemond JJ, Martin W. 2010. Acetate
768 formation in the energy metabolism of parasitic helminths and protists. Int J Parasitol
769 40:387-397.
770 68. Zaiss MM, Rapin A, Lebon L, Dubey LK, Mosconi I, Sarter K, Piersigilli A, Menin L,
771 Walker AW, Rougemont J, Paerewijck O, Geldhof P, McCoy KD, Macpherson AJ,
772 Croese J, Giacomin PR, Loukas A, Junt T, Marsland BJ, Harris NL. 2015. The intestinal
773 microbiota contributes to the ability of helminths to modulate allergic inflammation.
774 Immunity 43:998-1010.
775 69. Cantacessi C, Giacomin P, Croese J, Zakrzewski M, Sotillo J, McCann L, Nolan MJ,
776 Mitreva M, Krause L, Loukas A. 2014. Impact of experimental hookworm infection on
777 the human gut microbiota. J Infect Dis 210:1431-4.
778 70. Smith PM, Howitt MR, Panikov N, Michaoud M, Gallini CA, Bohlooly YM, Glickman
779 JN, Garrett WS. 2013. The microbial metabolites, short-chain fatty acids, regulate colonic
780 Treg cell homeostasis. Science 341:596-573.
781 71. Belzer C, Chia LW, Aalvink S, Chamlaqain B, Piironen V, Knol JC, de Vos WM. 2017.
782 Microbial metabolic networks at the mucus layer lead to diet-independent butyrate and
783 vitamin B12 production by intestinal symbionts. MBio 8:e00770-17.
784 72. Wong JM, de Souza R, Kendall CW, Emam A, Jenkins DJ. 2006. Colonic health:
785 fermentation and short chain fatty acids. J Clin Gastroenterol 40:235-243.
786 73. Greer JB, O'Keefe SJ. 2011. Microbial induction of immunity, inflammation, and cancer.
787 Front Physiol 1:168.
788 74. Scheppach W. 1994. Effects of short chain fatty acids on gut morphology and function.
789 Gut 35:S35-38.

790 75. Vinolo MAR, Rodrigues HG, Nachbar RT, Curi R. 2011. Regulation of inflammation by
791 short chain fatty acids. Nutrients 3:858-876.
792 76. Shepherd C, Giacomin P, Miller C, Navarro S, Loukas A, Wangchuk P. 2018. A
793 medicinal plant compound, capnoidine, prevents the onset of inflammation in a mouse
794 model of colitis. J Ethnopharmacol 211:17-28.
795 77. Overgaard AJ, Weir JM, De Souza DP, Tull D, Haase C, Meikle PJ, Pociot F. 2016.
796 Lipidomic and metabolomic characterization of a genetically modified mouse model of
797 the early stages of human type 1 diabetes pathogenesis. Metabolomics 12.
798 78. Wangchuk P, Keller PA, Pyne SG, Taweechotipatr M, Kamchonwongpaisan S. 2013.
799 GC/GC-MS analysis, isolation and identification of bioactive essential oil components
800 from the Bhutanese medicinal plant, *Pleurospermum amabile*. Nat Prod Commun 8:1308-
801 08.
802 79. Han J, Lin K, Sequeira C, Borchers CH. 2015. An isotope-labeled chemical derivatization
803 method for the quantitation of short-chain fatty acids in human feces by liquid
804 chromatography–tandem mass spectrometry. Anal Chim Acta 854:86-94.
805
806
807 **Figure legends**
808
809 **FIG 1.** Protective effects of intra-peritoneal administration of somatic tissue metabolite extracts
810 of *A. caninum* against different clinical symptoms of inducible colitis in mice (N = 10). (A)
811 TNBS-induced body weight loss. (B) mobility score. (C) piloerection score. (D) fecal consistency
812 score. (E) fecal pellet counts. Statistical analyses were performed using Graphpad Prism 7 (2way
813 ANOVA and unpaired and nonparametric Mann-Whitney t-test, *P < 0.05, **P < 0.01, ***P <
814 0.001, ****P < 0.0001).

FIG 2. Macroscopic pathology scores of mice treated with different somatic tissue LMWM extracts of *A. caninum* (N = 10)**.** (A) colon length shortening; (B) colon wall thickening; (C) number of adhesions; (D) extent of edema (E); degree of ulceration. Statistical analyses was performed using Graphpad Prism 7 (unpaired and nonparametric Mann-Whitney t-test, *P<0.05; **P<0.01; ***P<0.001; ****P<0.0001).

FIG 3. Administration of SE-HDA and SE-MeOH protects mice against TNBS-induced colonic inflammation. (A) Representative histological photomicrographs of haematoxylin and eosin-stained (H/E) paraffin sections (×200) of distal colon tissues of an untreated mouse with normal goblet cells (green arrow), lamina propria (black arrow) and colon wall (blue arrow); TNBS control mouse colon showed erosion of goblets cells (green arrow), thickening of lamina propria (black arrow), cell infiltration (red arrow) and colon wall thickening (blue arrow); mice treated with SE-HDA/TNBS and SE-MeOH/TNBS showed less pathology than the untreated TNBS only control group. Mice treated with SE-DCM/TNBS, SE-Acidic/TNBS and SE-Basic/TNBS extract were not protected against colitic immunopathology. (B) Scoring of histological outcomes of all treatment groups for pathological changes. Statistical analyses were performed using Graphpad Prism 7 (unpaired and nonparametric Mann-Whitney t-test, *P < 0.05).

FIG 4. Cytokine profile of mice treated with somatic tissue extracts of *A. caninum* (n = 10). (A) IFN-γ (P = 0.3538). (B) IL-17A (P = 0.1510). Statistical analyses were performed using Graphpad Prism 7 (unpaired and nonparametric Mann-Whitney t-test, P < 0.05 was considered significant).

839 **FIG 5.** Co-culture of human PBMC with *A. caninum*–derived SE-MeOH, SE-DCM and SE-HDA
840 at a final concentration of 20 µg/ml prior to stimulation with LPS resulted in significant
841 suppression of the pro-inflammatory cytokines IL-1β (A), IL-6 (B), TNF-α (C) and MCP-1 (D).
842 Statistical analyses were performed using Graphpad Prism 7 (unpaired t-test, **P < 0.001, ****P
843 < 0.0001)
844
845 **FIG 6.** Dose-response effect of inflammatory cytokine and chemokine secretion by human
846 PBMC in the presence of different concentrations of SE-HDA extract of *A. caninum*. Stimulation
847 with LPS resulted in significant suppression of the pro-inflammatory cytokines IL-1β (A), IL-6
848 (B), TNF-α (C), and MCP-1 (D). A multi-donor analysis showed SE-HDA induced significant
849 suppression of IL-1β (E) and MCP-1 (F) in all 6 donors. Statistical analyses were performed
850 using Graphpad Prism 7 (unpaired t-test, *P<0.05; **P<0.01; ***P<0.001; ****P<0.0001).
851

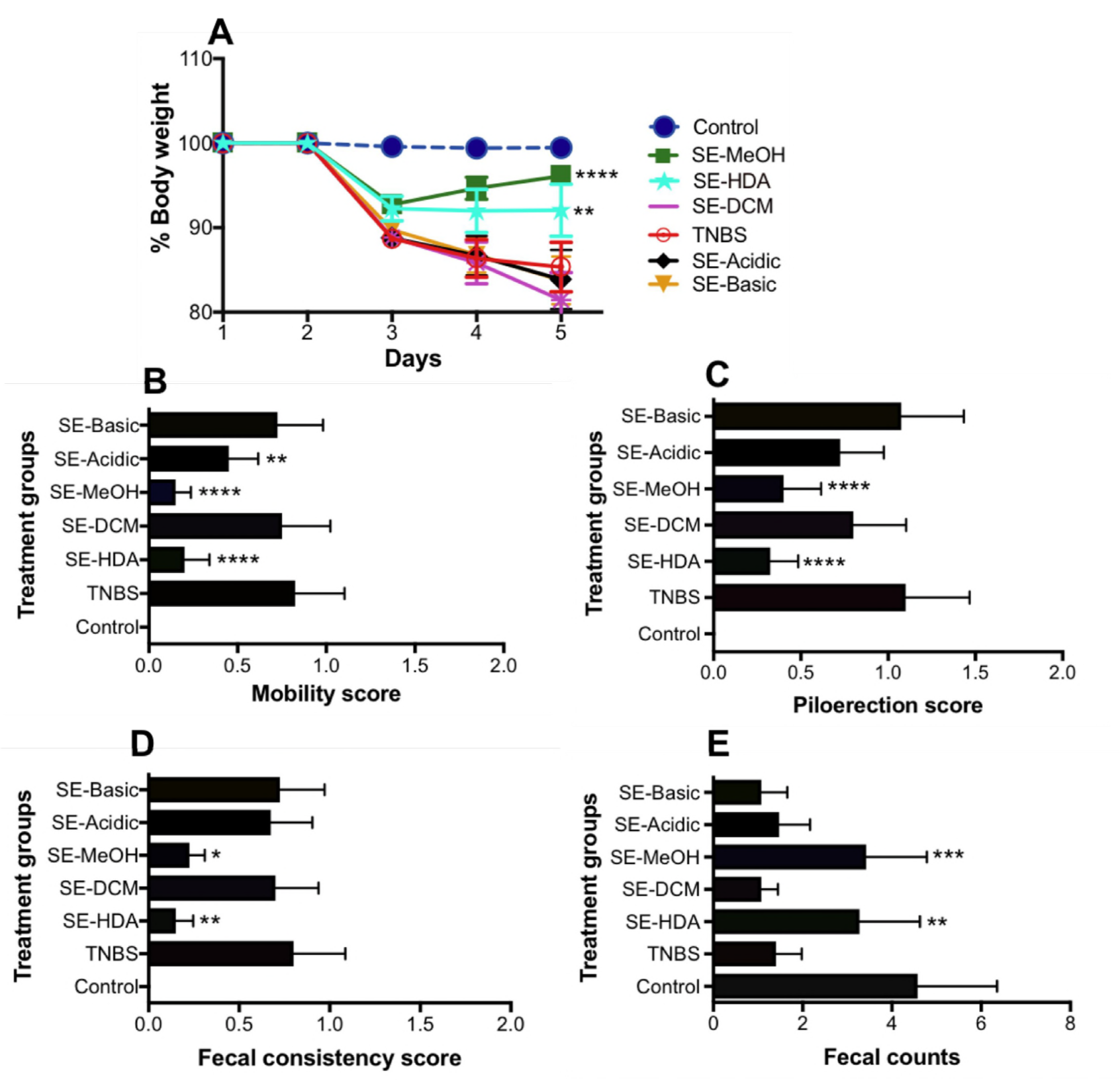
A
% Body weight
110
100
90
80
1
2
3
4
5
Days
****
**
Control
SE-MeOH
SE-HDA
SE-DCM
TNBS
SE-Acidic
SE-Basic
B
Treatment groups
SE-Basic
SE-Acidic
SE-MeOH
SE-DCM
SE-HDA
TNBS
Control
**
****
****
0.0
0.5
1.0
1.5
2.0
Mobility score
C
Treatment groups
SE-Basic
SE-Acidic
SE-MeOH
SE-DCM
SE-HDA
TNBS
Control
****
****
0.0
0.5
1.0
1.5
2.0
Piloerection score
D
Treatment groups
SE-Basic
SE-Acidic
SE-MeOH
SE-DCM
SE-HDA
TNBS
Control
*
**
0.0
0.5
1.0
1.5
2.0
Fecal consistency score
E
Treatment groups
SE-Basic
SE-Acidic
SE-MeOH
SE-DCM
SE-HDA
TNBS
Control
***
**
0
2
4
6
8
Fecal counts

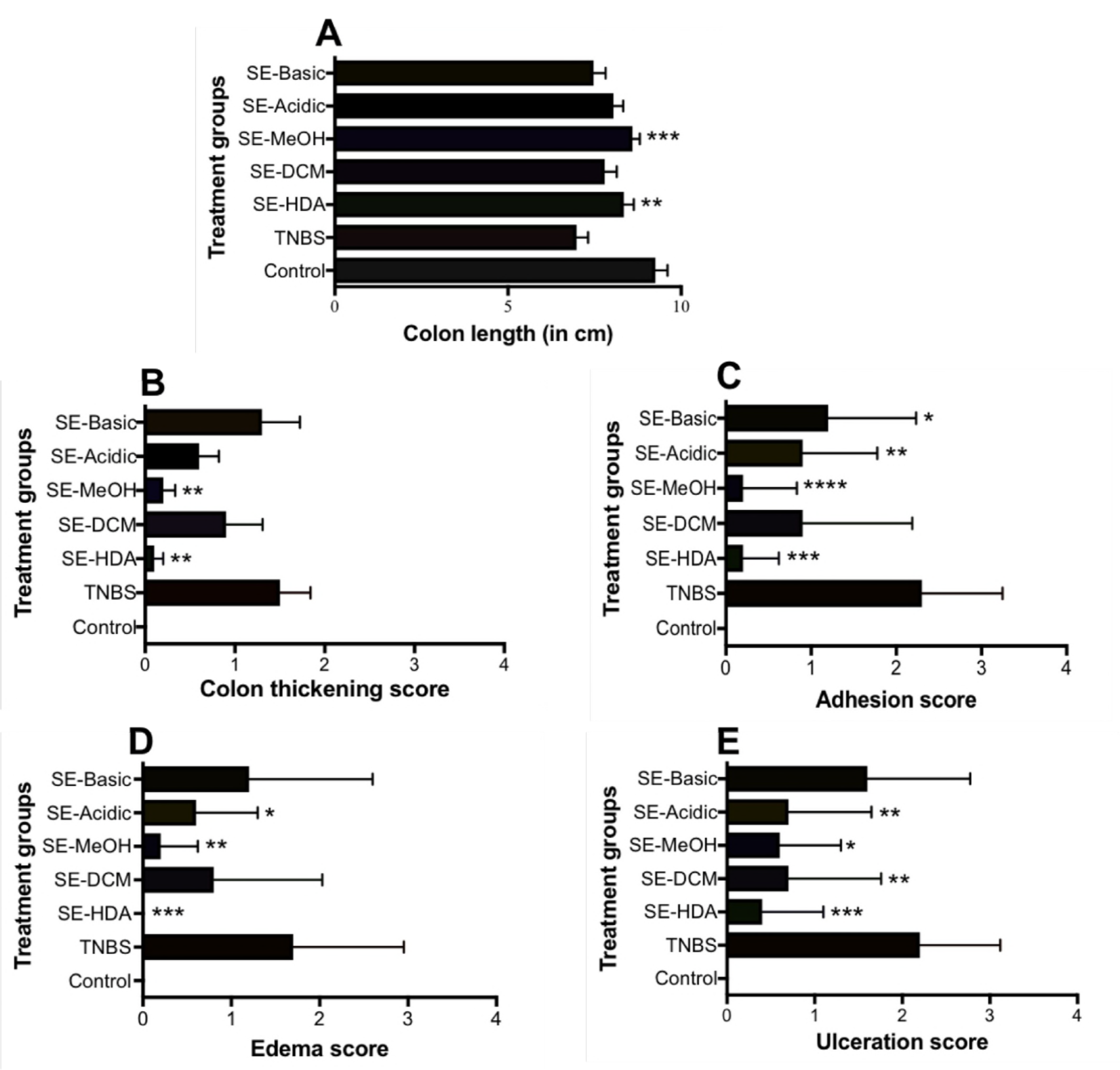
A
Treatment groups
SE-Basic
SE-Acidic
SE-MeOH
SE-DCM
SE-HDA
TNBS
Control
***
**
0
5
10
Colon length (in cm)
B
Treatment groups
SE-Basic
SE-Acidic
SE-MeOH
SE-DCM
SE-HDA
TNBS
Control
**
**
0
1
2
3
4
Colon thickening score
C
Treatment groups
SE-Basic
SE-Acidic
SE-MeOH
SE-DCM
SE-HDA
TNBS
Control
*
**
****
***
0
1
2
3
4
Adhesion score
D
Treatment groups
SE-Basic
SE-Acidic
SE-MeOH
SE-DCM
SE-HDA
TNBS
Control
*
**
***
0
1
2
3
4
Edema score
E
Treatment groups
SE-Basic
SE-Acidic
SE-MeOH
SE-DCM
SE-HDA
TNBS
Control
**
*
**
***
0
1
2
3
4
Ulceration score

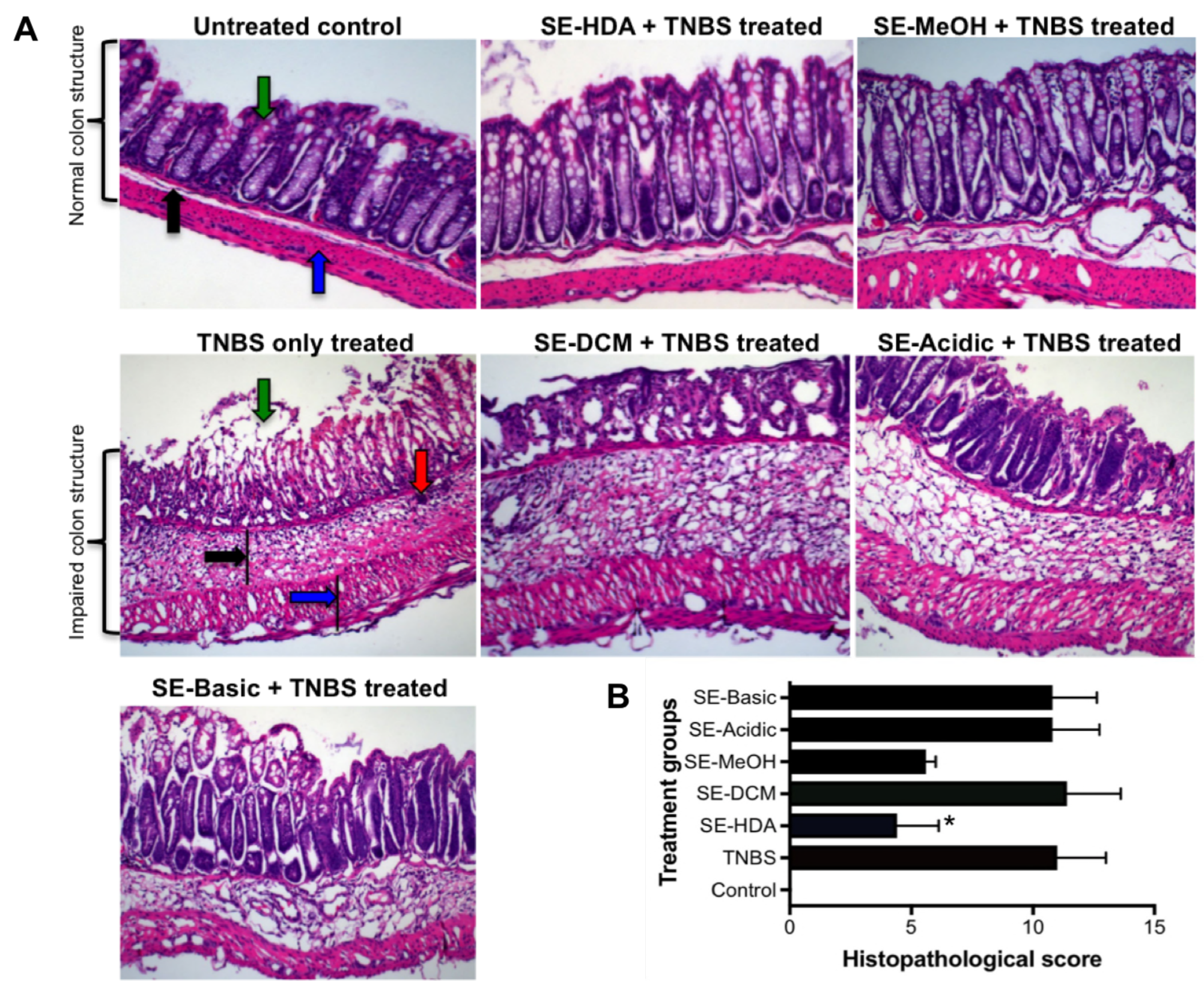
A
Untreated control
SE-HDA + TNBS treated
SE-MeOH + TNBS treated
Normal colon structure
TNBS only treated
SE-DCM + TNBS treated
SE-Acidic + TNBS treated
Impaired colon structure
SE-Basic + TNBS treated
B
Treatment groups
SE-Basic
SE-Acidic
SE-MeOH
SE-DCM
SE-HDA
TNBS
Control
*
0
5
10
15
Histopathological score

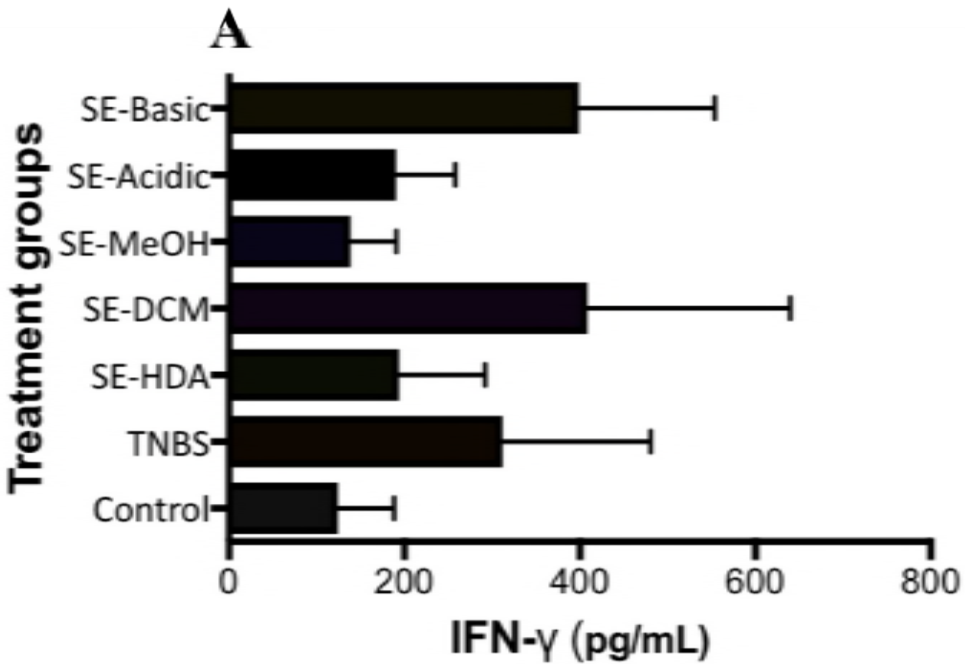
A
Treatment groups
SE-Basic
SE-Acidic
SE-MeOH
SE-DCM
SE-HDA
TNBS
Control
0
200
400
600
800
IFN-γ (pg/mL)

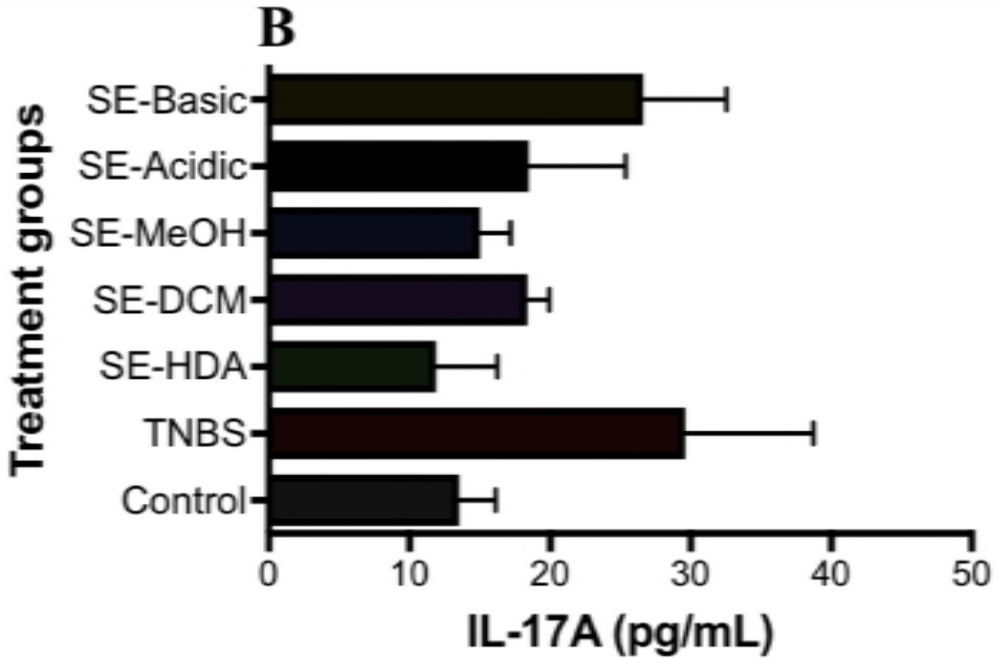
B
Treatment groups
SE-Basic
SE-Acidic
SE-MeOH
SE-DCM
SE-HDA
TNBS
Control
0
10
20
30
40
50
IL-17A (pg/mL)

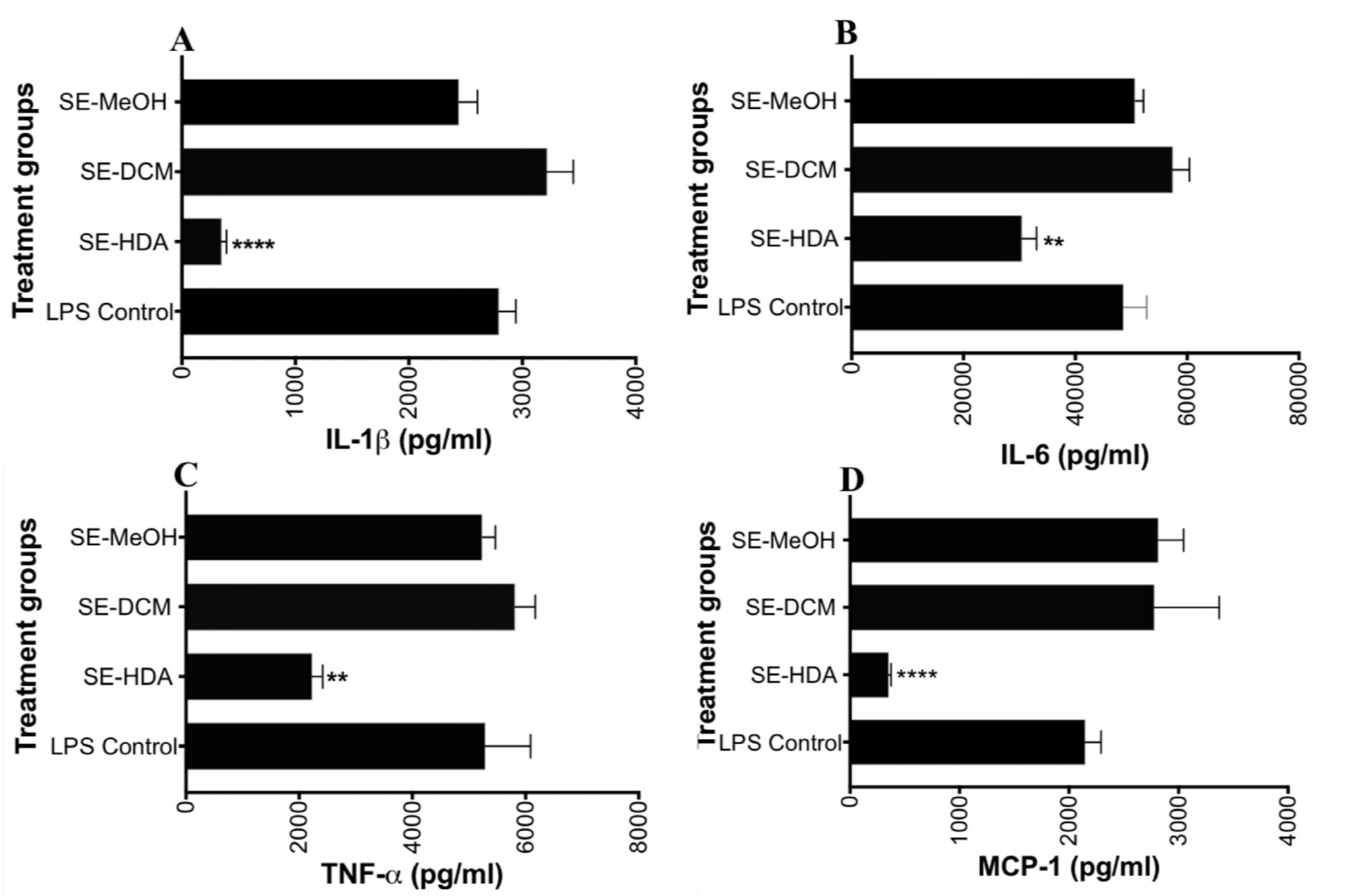
A
Treatment groups
SE-MeOH
SE-DCM
SE-HDA
LPS Control
****
0
1000
2000
3000
4000
IL-1β (pg/ml)
B
Treatment groups
SE-MeOH
SE-DCM
SE-HDA
LPS Control
**
0
20000
40000
60000
80000
IL-6 (pg/ml)
C
Treatment groups
SE-MeOH
SE-DCM
SE-HDA
LPS Control
**
0
2000
4000
6000
8000
TNF-α (pg/ml)
D
Treatment groups
SE-MeOH
SE-DCM
SE-HDA
LPS Control
****
0
1000
2000
3000
4000
MCP-1 (pg/ml)

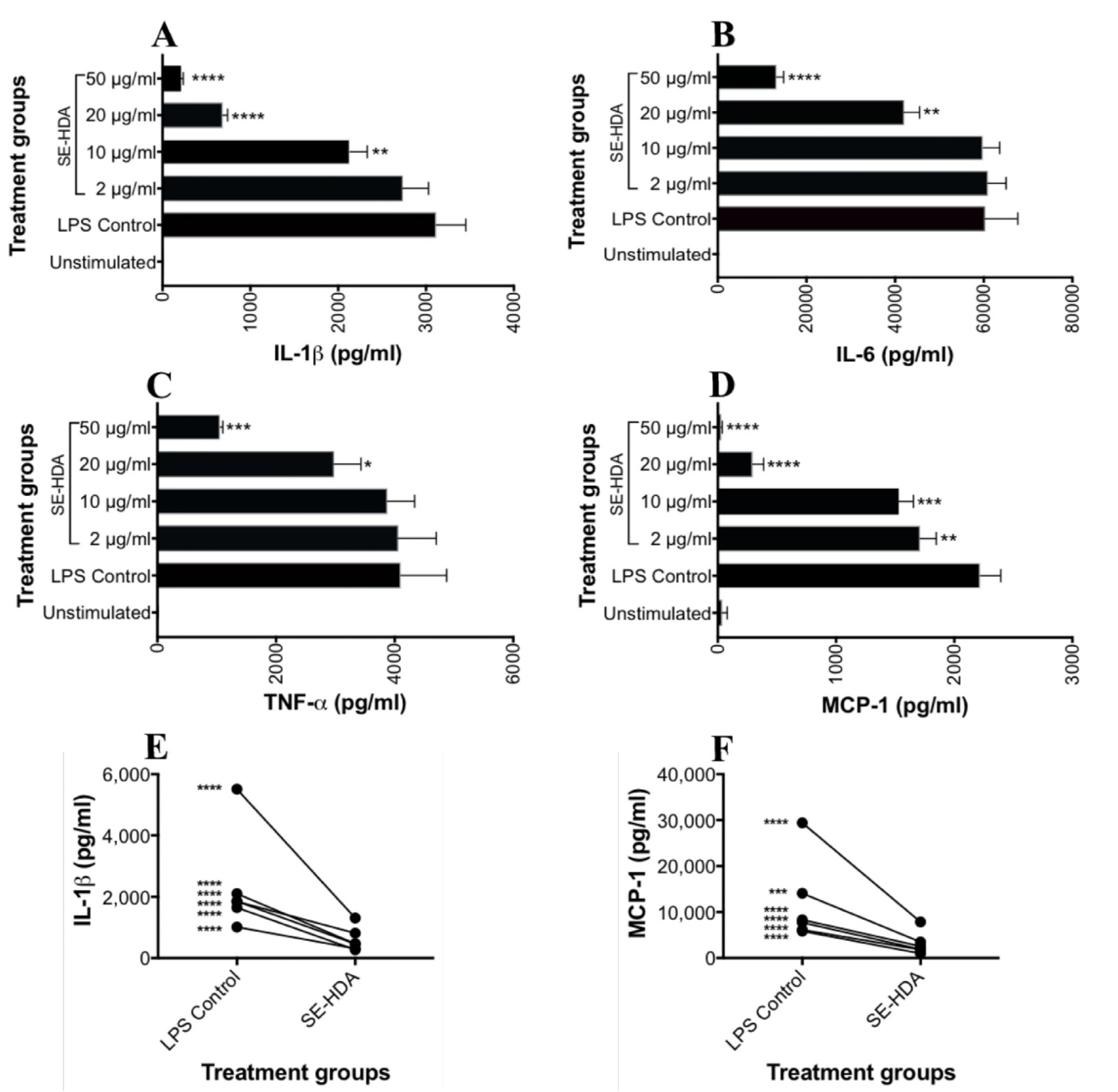
A
Treatment groups
SE-HDA
50 µg/ml
20 µg/ml
10 µg/ml
2 µg/ml
LPS Control
Unstimulated
****
****
**
0
1000
2000
3000
4000
IL-1β (pg/ml)
B
Treatment groups
SE-HDA
50 µg/ml
20 µg/ml
10 µg/ml
2 µg/ml
LPS Control
Unstimulated
****
**
0
20000
40000
60000
80000
IL-6 (pg/ml)
C
Treatment groups
SE-HDA
50 µg/ml
20 µg/ml
10 µg/ml
2 µg/ml
LPS Control
Unstimulated
***
*
0
2000
4000
6000
TNF-α (pg/ml)
D
Treatment groups
SE-HDA
50 µg/ml
20 µg/ml
10 µg/ml
2 µg/ml
LPS Control
Unstimulated
****
****
***
**
0
1000
2000
3000
MCP-1 (pg/ml)
E
IL-1β (pg/ml)
6,000
4,000
2,000
0
LPS Control
SE-HDA
Treatment groups
F
MCP-1 (pg/ml)
40,000
30,000
20,000
10,000
0
LPS Control
SE-HDA
Treatment groups